Pergamon

Scripta Materialia, Vol. 38, No. 4, pp. 667–674, 1998
Elsevier Science Ltd

1359-6462/98 $19.00 + .00

PII S1359-6462(97)00511-3

HIGH STRAIN RATE BEHAVIOR OF A SiC PARTICULATE REINFORCED Al_2O_3 CERAMIC MATRIX COMPOSITE

I.W. Hall and M. Guden*
Mechanical Engineering Department and *Materials Science Program, University of Delaware, Newark, DE 19716, USA

(Received September 16, 1997)

Introduction

The high strain rate deformation behavior of composite materials is important for several reasons. First, knowledge of the mechanical properties of composites at high strain rates is needed for designing with these materials in applications where sudden changes in loading rates are likely to occur. Second, knowledge of both the dynamic and quasi-static mechanical responses can be used to establish the constitutive equations which are necessary to increase the confidence limits of these materials, particularly if they are to be used in critical structural applications. Moreover, dynamic studies and the knowledge gained from them are essential for the further development of new material systems for impact applications.

In this study, the high strain rate compressive deformation behavior of a ceramic matrix composite (CMC) consisting of SiC particles and an Al_2O_3 matrix was studied and compared with its quasi-static behavior. Microscopic observations were conducted to investigate the deformation and fracture mechanism of the composite.

Materials and Experimental Procedure

The composite was manufactured by Lanxide® using the DIMOX™ process [1,2] in which molten metal wicks through a preform of ceramic reinforcing particles and is simultaneously oxidized. This CMC material has applications as a ceramic armor and the typical microstructure is shown in Fig. 1. The composite microstructure exhibits three components, namely, SiC reinforcement particles, interconnected ceramic matrix Al_2O_3, and remnant Al metal which had not oxidized during the manufacturing process. Pores were observed in many SiC particles as shown in Fig. 1 but they form in the SiC manufacturing process rather than in the process of making the composite. The pores ranged in size from approximately 0.05μm to 1μm. It has been proposed that the presence of the metallic Al phase (white) in the composite contributes to the work of fracture by absorbing a considerable amount of energy *via* crack bridging [2].

Dynamic compression tests were carried out using a Split Hopkinson Pressure Bar (SHPB, also referred to as a Kolsky Bar) and for quasi-static tests a screw-driven Instron machine was used. Detailed information on the present SHPB and data reduction in this technique are given elsewhere [3,4]. Cylindrical specimens 8.3 mm in diameter and 12.5mm in height were prepared by diamond core drilling from as-received plate-shaped CMC material. Some of the Instron tested specimens were strain

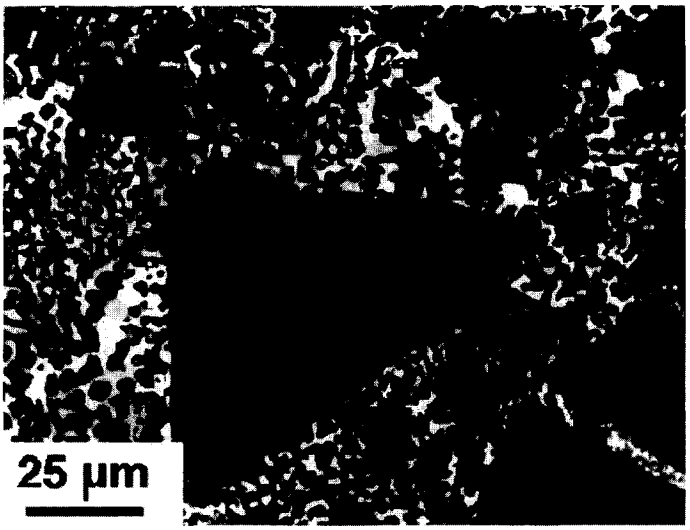

Figure 1. CMC microstructure showing SiC, Al_2O_3 and remnant metallic Al.

gaged in order to determine precisely Young's modulus and the fracture strain of the composite. The majority of specimens tested in the SHPB were strain gaged. It should be mentioned here that data from the SHPB in the initial several microseconds of the test can not be interpreted to show the correct material property response because of the absence of an equilibrium stress state in the sample. It has been shown previously that the stress in the sample closely approaches a uniform state after 4 or 5 wave reflections [5]. Hence, by multiplying by 5 the elastic wave transit time, which is specimen length divided by wave velocity, the lower (time) limit for stress equilibrium can be easily calculated for the composite. For ceramic materials the elastic wave velocity is on the order of 10,000ms^{-1}. Using this value, the lower limit may be calculated as 6μs so that before this time stress equilibrium is not established in the sample. In the highest strain rate tests attained in this study, samples fractured at a minimum of 15μs and this indicates that an acceptably uniform stress state was generally achieved in the present samples. In some of the SHPB tests, an aluminum pulse shaper was used to reduce the steepness of the incident wave and, hence, impose fracture of samples after several tens of microseconds. Typical stress strain curves are shown in Fig. 2.

Fractured samples were examined by scanning electron microscopy (SEM) and representative samples were also examined by transmission electron microscopy (TEM) before and after testing. Samples for the latter were prepared by conventional dimpling and ion milling procedures.

Results and Discussion

Samples tested at either quasi-static or high strain rates fractured at very low strains, typically 0.3–0.4%. Young's modulus of the composite was calculated from Instron tests with strain gaged samples and found to average 280GPa. The fracture stress at quasi-static strain rates was found to be ~900MPa. Previously, the compressive modulus and fracture stress of a similar composite were reported as 313GPa and 1193MPa respectively [2]. Although the present results are lower than values reported for a similar CMC, it should be noted that compression testing of ceramic materials are

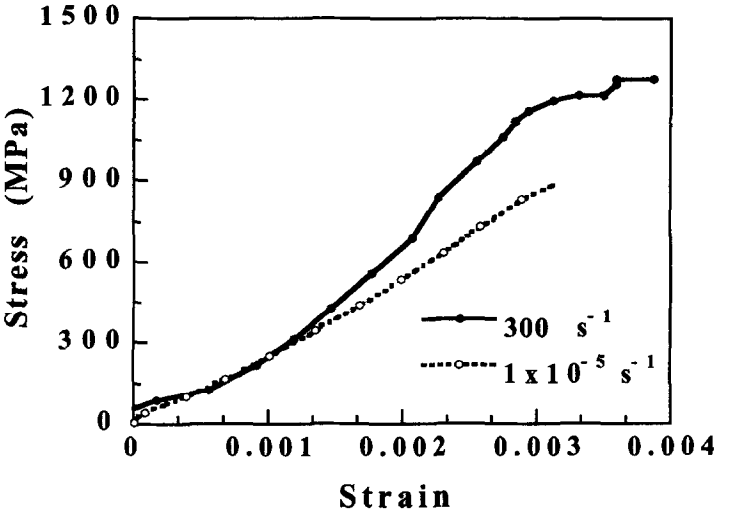

Figure 2. Typical high strain rate and quasi- static stress-strain curves.

influenced by the size and geometry of the sample. Also, the test fixture used in compression can strongly influence the measured fracture stress.

The highest strain rate attained in SHPB testing without using a pulse shaper was about $300s^{-1}$. Strain rates lower than this were obtained using a pulse shaper. A useful and common way of presenting strain rate effects in ceramics is to show the fracture stress as a function of the logarithm of strain rate. Such a graph for the tested composites is presented in Fig. 3. As noted from Fig. 3, the fracture stress of the composite increased as the strain rate increased beyond $\sim 100s^{-1}$. The fracture strain of the composite also increased slightly from 0.35 to 0.45% from quasi-static to high strain rates, respectively. Over the whole strain rate range investigated, the complete test data were found to fit best to a linear interpolation as:

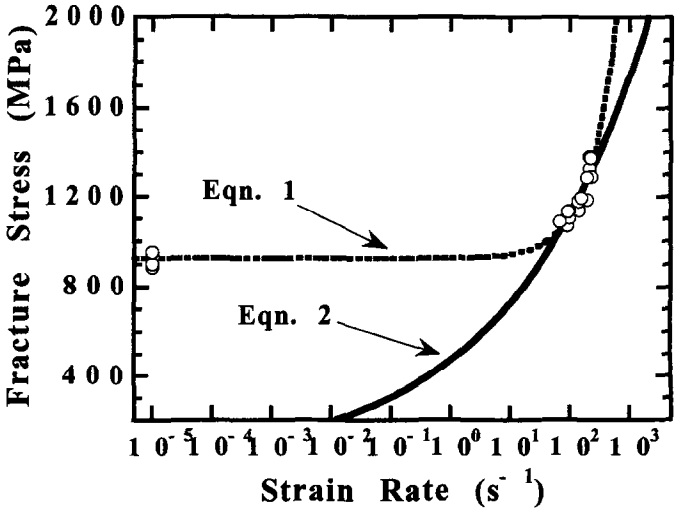

Figure 3. Fracture stress *vs.* logarithm of strain rate.

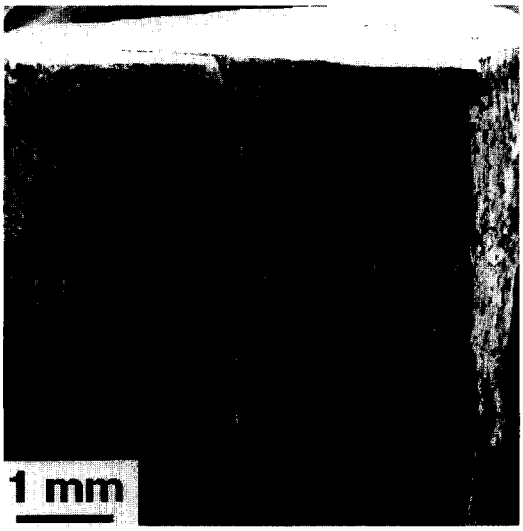

Figure 4. Large "slab" fragment from tested CMC. Compression axis vertical.

$$\sigma = 924 + 1.78 \times \dot{\varepsilon} \quad (1)$$

The high strain rate fracture stress data on their own ($>100s^{-1}$) were also subjected to a power law fit to the applied strain rate, thus:

$$\sigma = 466 \times \dot{\varepsilon}^{0.19} \quad (2)$$

Both these fits are shown in Fig. 3.

Regardless of the strain rate, fracture occurred on planes parallel to the compressive load axis and gave rise to several relatively large pieces, the general appearance of which is shown in Fig. 4. This type of fracture mechanism observed in brittle materials is called 'slabbing' and results from the propagation of microcracks to combine to give final failure [6]. Rigorously, the failure of ceramics under compression may be considered as crack initiation, propagation and linkage. The cracks in ceramic materials are usually initiated from inhomogeneities such as grain boundaries, cavities, inclusions and flaws [6, 7]. Microcracks nucleated under tension become parallel to the loading axis and undergo coalescence to form final failure.

Examination of the fracture surface of the composite revealed that cracks were initiated either from the pores within the SiC particles or at the external particle surfaces. The former event is illustrated by the crack surface in an SiC particle shown in Fig. 5 where, first, the fracture is seen to be of the cleavage type and, second, the crack path interacts with and follows porosity sites during propagation. The cracks in SiC particles subsequently penetrate into the Al_2O_3 matrix (or *vice versa*), however, the growth of cracks in the matrix appeared to be effectively stopped by a combination of the small grain size and the presence of a small volume fraction of ductile Al phase. A typical fracture surface through both a SiC particle and the matrix is presented in Fig. 6 where the SiC/Al_2O_3 interface is clearly seen. This micrograph also shows that many of the small Al_2O_3 particles in the matrix are located in the ductile dimples created by plastic deformation and necking of the remnant metallic aluminum of the matrix: this phenomenon indicates an important crack arrest or hindering mechanism. In addition, many of the SiC particles themselves showed wavy and serrated surface features which most likely correspond to activation of multiple intersecting cleavage planes due to the presence of many crystallographic polytypes of SiC present in each particle, Fig. 7. The wavy lines may also possibly arise due to plastic

Figure 5. Crack propagation from porosity in SiC particle.

deformation processes but they greatly increase the surface area and, therefore, constitute important energy absorption mechanisms whatever their cause. Final failure of the composite occurred by coalescence of these microcracks and catastrophic propagation.

TEM studies confirmed the general structure shown in Fig. 1, showing large crystalline particles of SiC, relatively small crystallites of Al_2O_3, and small ($\sim 1\mu m$) areas of metallic Al. However, several differences of note were observed between untested and tested samples. First, the metallic aluminum was present in untested samples as small, single crystal grains with very low dislocation density. This structure corresponds with what would be expected from the high temperature molten metal infiltration production route in giving rise to well-annealed single crystals. However, after testing, the aluminum grains invariably showed a clearly defined subgrain structure with well defined cell walls, a subgrain

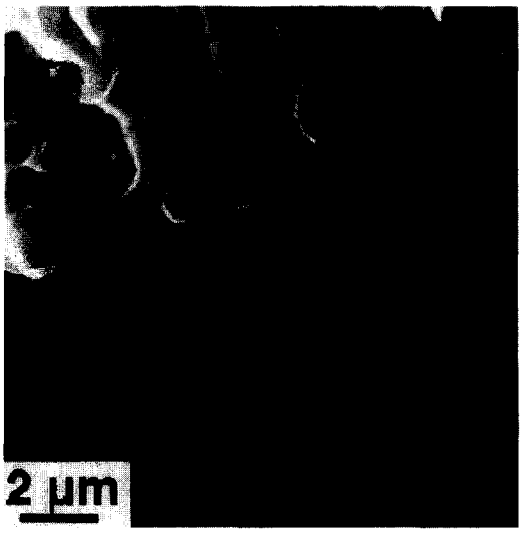

Figure 6. Fracture at SiC/matrix interface showing (at top) dimples in metallic Al.

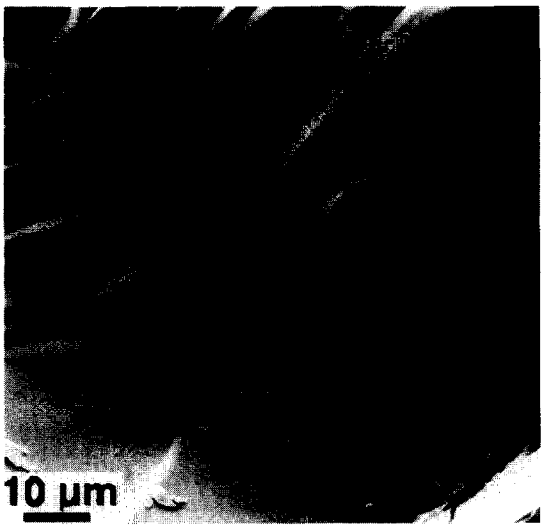

Figure 7. Serrated fracture surface of SiC due to activation of multiple cleavage planes.

size of 0.1 μm, and a high remnant dislocation density. Untested and tested structures are illustrated in Figs. 8(a) &(b). The most probable interpretation of these structures is that they are consistent with the aluminum having been heavily plastically deformed during the test, and that the deformation was sufficient to induce recovery and/or recrystallization during or immediately after the compression test. The clear demonstration that the aluminum has undergone severe plastic deformation is strong supporting evidence for its important role in the crack arrest processes referred to above.

The second significant observation concerned the SiC particles themselves. After testing, many of the particles were cracked and extensive dislocation arrays were almost invariably noted at the crack tip, Fig. 9. This is further evidence that, although generally regarded as brittle, the SiC can itself absorb considerable energy in fracture, especially if constrained to some extent by a matrix which inhibits extensive and rapid fracture.

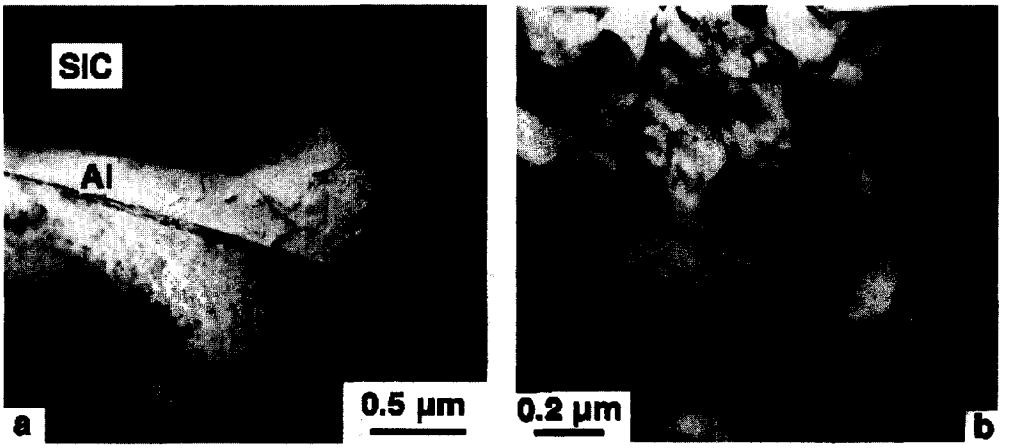

Figure 8. (a). TEM micrograph showing metallic aluminum in untested CMC. (b). Recovery and/or recrystallization in Al of tested CMC. (TEM micrograph)

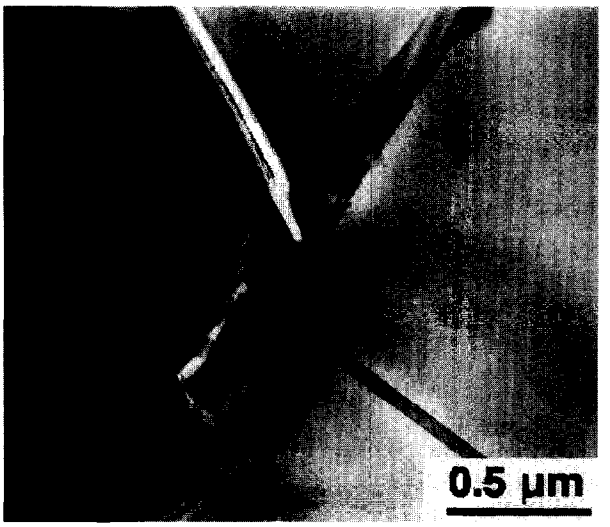

Figure 9. TEM micrograph showing dislocation generation at crack tip in SiC.

Increased fracture stress with increasing strain rate is widely observed in monolithic and composite ceramic materials [8–10]. The increased fracture stress in brittle materials with increasing strain rate is attributed to inertia-dominated dynamic crack growth from pre-existing flaws. It is argued that the cracks are initiated athermally and, once nucleated, the rate controlling process is inertia which is suggested to be independent of material properties [10]. Based on this argument, it is suggested that the fracture stress in the high strain rate regime is given as [11]:

$$\sigma \propto \dot{\varepsilon}^{1/3} \tag{3}$$

This dependence of fracture stress prevails after a critical strain rate [8]. The critical strain rate for monolithic ceramic materials such as Al_2O_3, SiC and AlN is found to be around $1000s^{-1}$ [8,10]. The observed lower transition strain rate in this composite may be attributed to the relatively larger size of pores which may reduce the critical strain rate [7]. As stated above, the interpolation of experimental data given in Fig. 3 gave a strain rate exponent of ~0.2 (Eqn. 2) which is smaller than the proposed exponent of 0.33.

The outstanding properties of the material as an armor can thus be understood in terms of its strain rate sensitivity and its microstructure. The strain rates measured here were in the range from quasi-static to $\sim 300s^{-1}$, whereas strain rates under ballistic impact conditions may exceed this by a factor of 10^2. At these strain rates, using data from the present tests, the fracture stress of the composite may be calculated as >54GPa (Equation 1), or 3.3GPa (Equation 2). Although there is no reason *a priori* to accept either of these major extrapolations at face value, it is clear that the fracture stress at ballistic strain rates is going to be significantly higher than the values measured here.

In addition to confirming plastic deformation in the SiC, it is believed that this work has shown for the first time that the remnant metallic aluminum in the CMC undergoes significant plastic deformation during fracture of the composite. This work has shown, therefore, that both the Al and the SiC can deform and absorb energy, thus providing major increments of energy absorption.

Conclusions

A CMC consisting of SiC particles in an alumina matrix has been compression tested at quasi-static and high strain rates. The measured low compression fracture strain and stress of the composite may be attributed to the many large pores in the SiC reinforcement. Failure of the composite was observed to be initiated from pores and propagated through the matrix until axial splitting of the composite. Several microstructural observations of fracture surface were presented. The observed increased fracture stress in high strain rate ($\sim 10^2 s^{-1}$) was reasonably well in accord with the well known phenomenon of inertia dominated crack propagation in brittle materials. The ballistic penetration resistance of the material is explained in terms of its strain rate sensitivity and microstructural factors.

Acknowledgments

The authors gratefully acknowledge the provision of the material used in this study by Lanxide Armor Products, Inc., Newark, Delaware. Financial support from the Army Research Office (award #DAAH04-95-2-0001) and a fellowship (M.G.) from the Izmir Institute, Turkey, are also gratefully acknowledged.

References

1. M. S. Newkirk, H. D. Lesher, D. R. White, C. R. Kennedy, A. W. Urquhart, and T. D. Claar, Ceram. Eng. Sci. Proc. 8, 879 (1987).
2. DoD Metal Matrix Composites Information Analysis Center, Current Highlights, Vol. 9, No. 3, September (1989).
3. M. Guden and I. W. Hall, Mater. Sci. Engnr. A232, 1 (1997).
4. P. S. Follansbee, Metals Handbook 8, pp.198–203, ASM, Metals Park, OH (1985).
5. D. J. Parry, P. R. Dixon, S. Hodson, and N. Al-Maliky, J. de Phys. IV. 4, C8–107 (1994).
6. M. F. Ashby and S. D. Hallam, Acta Metall. Mater. 34, 497 (1986).
7. S. Nemat-Nasser and H. Deng, Acta Metall. Mater. 42, 1013 (1994).
8. J. Lankford, Comm. Amer. Ceram. Soc. C-33 (1981).
9. J. Lankford and C. R. Blanchard, Mater. Sci. Engnr. A138, 63 (1991).
10. G. Ravichandran and G. Subhash, Int. J. Solids Structures. 32, 2627 (1995).
11. D. E. Grady and J. Lipkin, Geophys. Res. Lett. 7, 255 (1980).